HHS Public Access

Author manuscript

J Neural Eng. Author manuscript; available in PMC 2021 December 23.

Published in final edited form as:

J Neural Eng. ; 17(5): 056009. doi:10.1088/1741-2552/abb7a6.

Chronic intracochlear electrical stimulation at high charge densities: Reducing platinum dissolution

Robert K. Shepherd[1,2], **Paul M. Carter**[3], **Ya Lang Enke**[3], **Alex Thompson**[1,2], **Brianna Flynn**[1], **Ella P. Trang**[1], **Ashley N. Dalrymple**[1,4], **James B. Fallon**[1,2]

[1]Bionics Institute, St Vincent's Hospital, Melbourne, Australia

[2]Medical Bionics Department, The University of Melbourne, Melbourne, Australia

[3]Cochlear Ltd., Sydney, Australia

[4]Department of Physical Medicine and Rehabilitation, University of Pittsburgh, Pittsburgh, PA, USA

Abstract

Objective: Histological examination of cochleae from long-term cochlear implant users has shown evidence of particulate platinum (Pt) corroded from the surface of Pt electrodes. The pathophysiological effect of Pt within the cochlea has not been extensively investigated. We previously evaluated the effects of Pt corrosion *in vivo* using biphasic current pulses at high charge densities (≥ 267 μC/cm^2/phase) and charge recovery using electrode shorting and found negligible pathophysiological impact. The present study extends this work by examining techniques that may reduce Pt corrosion.

Approach: Deafened guinea pigs were continuously stimulated for 28 days using biphasic current pulses at extreme charge densities of up to 540 μC/cm^2/phase using: (i) electrode shorting; (ii) electrode shorting with capacitive coupling (CC); or (iii) electrode shorting with alternating leading phase (AP). On completion of stimulation, cochleae were examined for corrosion product, tissue response, auditory nerve (AN) survival and trace levels of Pt; and electrodes examined for evidence of surface corrosion.

Main results: Cochleae stimulated at ≥ 228 μC/cm^2/phase showed particulate Pt, the extent of which was dependent on both charge density ($p < 0.01$) and charge recovery technique ($p < 0.01$); reduced Pt was evident in cochleae stimulated using CC or AP. Stimulation at charge densities ≥ 200 μC/cm^2/phase resulted in significant electrode corrosion ($p < 0.05$); which was reduced using CC. Trace levels of Pt was reduced in cochleae stimulated with the addition of CC. Tissue response within cochleae increased with charge density ($p < 0.007$); cochleae stimulated at ≥ 200 μC/cm^2/phase exhibited a vigorous response including a focal region of necrosis and macrophages. Notably, tissue response was not dependent on the charge recovery technique ($p = 0.56$). Finally, despite stimulation at high charge densities resulting in significant levels of Pt corrosion, there was no stimulus induced loss of ANs.

Corresponding Author: Prof Robert Shepherd, Bionics Institute, St Vincent's Hospital, 41 Victoria Parade, Fitzroy, VIC 3065, Australia, rshepherd@bionicsinstitute.org.

Significance: Significant increases in tissue response and Pt corrosion were observed following stimulation at high charge densities. Charge recovery using CC, and to a lesser extent AP, reduced the amount of Pt corrosion but not the tissue response. Despite chronic stimulation at change densities which are an order of magnitude higher than those used when programming cochlear implant recipients in the clinic, producing a vigorous tissue response and Pt corrosion products, there was no evidence of a stimulus induced loss of neurons.

Keywords

Electrical stimulation; neural prosthesis; platinum electrode; stimulation safety; corrosion; tissue response

2. Introduction:

Platinum (Pt) is the most common electrode material used in commercial neural prostheses (1). It has a long history of clinical use and is regarded as a safe electrode material when used in combination with carefully controlled charge-balanced current pulses operating within stimulus levels that allow charge injection via reversible Faradaic reactions (2, 3). However, recent studies examining cochleae from patients that were long-term cochlear implant users during their life-time have shown evidence of particulate Pt within the tissue capsule surrounding the electrode array (4–7). Some of these clinical reports also described an increased foreign body response associated with the particulate Pt (6, 7).

We recently demonstrated in an animal model of cochlear implantation, that four weeks of continuous stimulation using high charge densities (267 & 400 μC/cm^2/phase); approximately an order of magnitude greater than typical clinical levels (median bipolar: 50 μC/cm^2/phase; monopolar: ~10 μC/cm^2/phase), resulted in significant amounts of particulate Pt within the tissue capsule proximal to the electrode array (8). Notably, the generation of this corrosion product was not associated with an increased loss of primary auditory neurons (ANs). The extent of the foreign body response was dependent on charge density; cochleae stimulated at 267 or 400 μC/cm^2/phase exhibited an extensive tissue response that included a focal region of necrosis close to the electrode. In contrast, cochleae stimulated at 100 μC/cm^2/phase showed no clear evidence of Pt corrosion and only a minimal tissue response.

Safe electrical stimulation of neural tissue is achieved by the creation of a capacitive layer at the electrode–tissue interface known as the Helmholtz double layer, and a series of electrochemical reactions that convert the charge carriers from electrons (in the electrode) to ions (in the electrolyte) (3, 9, 10). At low charge densities (<20 μC/cm^2/phase), the charge injection process is dominated by capacitive mechanisms; no charge carrier physically crosses the electrode–tissue interface and therefore no electrochemical reaction products are formed within the electrolyte (11, 12). As the charge density is increased, reversible electrochemical Faradaic reactions begin to dominate the charge injection process, including oxide formation/reduction and hydrogen-atom plating (3, 9). Importantly, these reactions are localized to the electrode–tissue interface and can be readily reversed via the passage of an equal charge of opposite polarity - the charge-balanced biphasic pulse – ensuring that no new electrochemical species are released into the biological environment (9, 11,

12). At higher charge densities, charge injection is increasingly achieved via a number of irreversible electrochemical reactions, resulting in the release of electrode corrosion products, electrolysis of water, and oxidation of chloride ions (11). These electrochemical reaction products diffuse from the electrode and cannot be reversed, resulting in direct current (DC) if the anodic and cathodic irreversible by-products are not equal (13). The formation of electrode corrosion products (8, 14), local pH changes (15, 16), the formation of reactive oxygen species and tissue damage (17), can also occur. Protection against charge imbalance is usually achieved in clinical settings by shorting electrodes between current pulses and/or the use of electrode shorting with coupling capacitors (CCs)(18).

We have previously shown that electrode shorting with CC (13) and electrode shorting with alternating leading phase (AP) (15) can reduce residual DC levels *in vivo*. In the present study we compared the use of electrode shorting alone, with electrode shorting and CC, and electrode shorting and AP in a series of chronic stimulation studies using a wide range of charge densities (0, 100, 200, 228, 267, 400 or 540 $\mu C/cm^2$/phase) and stimulus rates (200 or 1000 pulses per second (pps)). We show that the level of Pt corrosion within stimulated cochleae is highly dependent on charge density, while the use of electrode shorting with CC, and to a lesser extent electrode shorting with AP, appears to reduce Pt corrosion. Tissue response within the implanted cochlea is also significantly dependent on charge density; however, it is *not* related to the extent of Pt corrosion product within the cochlea. Finally, despite chronic stimulation at charge densities which are an order of magnitude higher than those used when programming cochlear implant recipients in the clinic, producing a vigorous tissue response and Pt corrosion products, there was no evidence of neural loss. The present findings have implications for both cochlear implants and other neural prostheses that use Pt electrodes.

3. Methods:

The majority of the methods used in the present study have been described in detail in (8) and are therefore only briefly described here.

Experimental subjects

This study was performed using a total of 24 pigmented guinea pigs. Additional data from the 19 animals described in our previous study (8) were included in the present analysis resulting in a total of 43 animals. These animals are identified in Table 1. All procedures were conducted with approval from the Bionics Institute Animal Research and Ethics Committee, were performed in accordance with the Australian Code of Practice for the Care, and Use of Animals for Scientific Purposes (8^{th} Edition, 2013) and followed the principles of the US National Institutes of Health guidelines regarding the care and use of animals for experimental procedures.

Auditory brainstem responses

All animals had normal hearing and otoscopically normal tympanic membranes. Hearing status was determined by a click-evoked auditory brainstem response (ABR; threshold <50 decibels peak equivalent sound pressure level [dB p.e. SPL] re 20 μPa). Under general

anaesthesia (1–2% isoflurane in oxygen, 1L/min; Isoflo; Zoetis, UK), ABRs were recorded differentially using subcutaneous (s.c.) needle electrodes (vertex positive; neck negative; thorax ground). Acoustic clicks were presented at intensities from 100 dB p.e. SPL to below threshold (the smallest click amplitude required to evoke a peak-trough response of > 0.5 μV).

Deafening protocol

Under general anaesthesia (1–2% isoflurane), an intravenous injection of frusemide (130 mg/kg; Ilium, Australia) was delivered to the right jugular vein, followed by kanamycin sulfate (420 mg/kg, s.c.; Sigma-Aldrich, USA), producing a highly symmetrical bilateral sensorineural hearing loss (19). Seven days following this deafening procedure the hearing status of each animal was re-tested. Only animals that exhibited at least a 50 dB increase in threshold in both ears were included in this study.

Scala tympani electrode array

HL8 electrode arrays (Cochlear Ltd., Australia) were used in the present study. The array contains 8 half-band Pt electrodes (Fig. 1) with electrode 1 (E1) the most basal and electrode 8 (E8) the most apical. Each Pt electrode was connected via a leadwire to a battery powered stimulator (details below) located in a backpack.

Charge per phase was held constant (0.2 μC/phase) while charge density was controlled by varying the geometrical surface area of the Pt electrode contacts on the array. Each electrode array had exposed Pt contact areas of either 0.2, 0.1, 0.0875, 0.075, 0.05 or 0.0375 mm^2 manufactured via laser ablation of a region of polydimethylsiloxane (PDMS) overlaying each Pt electrode. The charge density associated with these electrode arrays were fixed at 100, 200, 228, 267, 400 or 540 $\mu C/cm^2$/phase respectively, for the duration of the stimulation program.

Cochlear implant surgery

Two weeks following deafening each animal was anaesthetized with isoflurane (2–2.5% in oxygen [1L/min]). Surgery was performed under aseptic conditions with the animal's temperature maintained at 37°C. A dorsal bulla approach was used to expose the left cochlea. The round window membrane was incised and the electrode array inserted into the scala tympani so the tip of the array was located in the upper basal turn (8). The round window was sealed, the leadwire fixed using dental cement (Duralon; Germany), and the distal leadwire tunnelled subcutaneously to exit the skin in the back of the neck. The wounds were sutured in two layers with Coated Vicryl 3–0 (Ethicon Inc., USA), and the animal was administered Hartmann's solution (10ml/kg; s.c.), Baytril (0.10mg/kg, s.c.; Bayer, Germany), and Temgesic (50 mg/kg, s.c.; Reckitt-Benckiser, UK). No surgery was performed on the right cochlea; they served as deafened, untreated controls.

Electrode impedance

The voltage transient impedance of each electrode on the array was measured in both a common ground and a bipolar configuration periodically during the chronic stimulation

period (20). The impedance was monitored by delivering a 100 μA biphasic current pulse of 100 μs pulse-width and recording the peak of the voltage transient during the first phase.

Electrically-evoked auditory brainstem responses

Electrically-evoked auditory brainstem responses (EABRs) were recorded to monitor AN function. EABRs were recorded intra-operatively and on completion of the 28 day stimulation program using the same recording configuration as ABRs (21). Biphasic current pulses (100 μs per phase; 50 μs interphase gap) were used to stimulate selected bipolar electrodes along the intracochlear electrode array (E1–E2, E2–E3, E3–E4, E4–E5, E5–E6, E6–E7, E7–E8). One hundred presentations were averaged for each recording. Two sets of recordings were made at each current level. Recordings were made at intensity intervals presented randomly from below threshold to a maximum of 250 Current Level (CL; where current in mA = $17.5 \times (100^{(CL/255)})$).

Chronic stimulation program

Immediately following the intra-operative EABR recordings each animal commenced a chronic stimulation program using a custom built back-pack stimulator (22) that delivered 100 μs/phase charge-balanced biphasic current pulses at 200 or 1000 pps at a charge/phase of 0.2 μC/phase via a tripolar electrode configuration (8). Animals were stimulated continuously over the 28 day implantation period. A cathodic first phase current was delivered to the centre electrode of the tripole while the two flanking electrodes provided the return path. All currents were then reversed in the second phase. Tripolar configuration was used as it allowed high charge levels to be used while maintaining comfortable levels of loudness. In the present study, centre electrodes generated charge densities of 100, 200, 228, 267, 400 or 540 μC/cm^2/phase (E4 and E7; Table 1), spanning a range of charge densities both within and significantly greater than the maximum recommended industry standard of 216 μC/cm^2/phase (23); while the flanking electrodes developed approximately half the charge density of the centre tripole electrode (E3, E5; E6 and E8; Table 1). Two electrodes on each array (E1 & E2) served as unstimulated control electrodes.

While charge-balanced current pulses significantly reduce the level of potentially damaging DC, stimulators typically use additional techniques in order to minimise any residual DC component. In the present study, charge-balance was achieved using one of three techniques (Table 1): (i) stimuli for cohorts 2–5 and 8 were charge-balanced using electrode shorting between current pulses (18), whereby electrodes are shorted together at a time when no current is delivered to ensure that any net charge during the previous stimulation pulse is recovered, a technique that was used exclusively in our previous study (8); (ii) cohorts 7 & 9 used both electrode shorting and CC, where 1 μF capacitors were placed in series with each electrode between the stimulator current source and the electrode contact; and (iii) cohort 6 used electrode shorting with AP – i.e. the polarity of the leading phase was alternated for each current pulse.

If stimulation using the tripolar configuration was not possible, for example due to high electrode impedance (> 25 kΩ) or lead wire breakage, stimulation of that tripolar electrode ceased.

Histology

On completion of the stimulation program all animals were euthanized with sodium pentobarbitone and systemically perfused with heparinised normal saline at 37°C, followed by 10% neutral buffered formalin at 4°C. The electrode array was removed for examination under a scanning electron microscope (SEM; see below). Both the stimulated and contralateral control cochleae were postfixed, decalcified, frozen, and sectioned at 12μm to the mid-modiolar point using a CM 1900 UV cryostat (Leica, Germany) at −22°C. The remaining half of the cochlea was kept for trace analysis of Pt using inductively coupled plasma mass spectrometry (ICP-MS; see below; (8)).

A representative series of cochlear sections were stained with haematoxylin and eosin (H&E) for qualitative examination (24). AN survival, measured as neural density, and the foreign body tissue response within the scala tympani were quantified. ANs were counted in mid-modiolar sections using a Zeiss Axioplan microscope by a single observer blinded to the experimental cohorts. ANs were identified within Rosenthal's canal and counted within the lower basal (LB), upper basal (UB), lower middle (LM), upper middle (UM) and the apical (A) cochlear regions (8, 24). Only ANs exhibiting a clear nucleus were counted. The area of Rosenthal's canal was measured using Image J software and the density of the ANs was determined. The AN density for each cochlear region was averaged from 5 sections that were spaced at least 72 μm apart, ensuring that no AN was counted more than once.

In order to quantify the foreign body response, the extent of fibrosis in the cochlea was measured in H&E stained sections at six locations along the electrode array (two each in the LB, UB and LM turns). An image of the scala tympani was captured and its area measured. The 'Triangle' algorithm in Image J was used to automatically threshold the image in order to quantify the tissue response. The area of scala tympani excluding the area of the electrode array was measured and the proportion of the scala tympani occupied by the tissue response calculated.

In addition to quantifying the extent of the tissue response in implanted cochleae, the nature of the inflammatory response adjacent to the electrode array was carefully examined and the extent of any necrotic and/or dense macrophage response was assessed by measuring the thickness of these zones in the section of each cochlea displaying the most extensive response (e.g. Fig. 2). Histological images were digitized using a Zeiss AxioLab microscope and the zone thickness measured using Image J software.

If present, the necrotic zone was identified by the presence of amorphous material and was surrounded by a band of cells including macrophages and plasma cells (8). The macrophage zone was typically surrounded by mature fibrous tissue that occupied large regions of the lumen of the scala tympani.

Each cochlea was also examined for evidence of electrode insertion trauma. All histological sections were examined under a microscope by a researcher experienced in cochlear histopathology. Insertion trauma was identified by fracture of the osseous spiral lamina and/or tears to the basilar membrane or the outer cochlear wall. This form of trauma evokes

a clear histopathological signature including a vigorous tissue response; neo-osseogenesis; loss of auditory neurons and an increased acute inflammatory response (25, 26).

Finally, each cochlea was also examined histologically for the presence of dense particulate material observed within the tissue capsule (8). The extent of this material was qualitatively graded from 0 – 4 (0, no evidence of particulate material in any section; 1, possible particulate material present; 2, clear localised particulate material present; 3, particulate material present in a number of sections; 4, widespread particulate material present).

Scanning Electron Microscopy

Following removal from the cochlea, each electrode array was rinsed, ultrasonically cleaned in distilled water, then stored in 70% ethanol. A small number of electrode arrays required additional cleaning in Enzol (diluted 1:40 for 1 hour at room temperature; WPI Inc, USA) to remove organic matter and allow examination of the underlying Pt electrode surface. All electrodes were examined using a FEI QUANTA 200 SEM and photographed at low (× 600) and medium (× 2000) magnification. A region of each electrode surface was then randomly selected and photographed at higher magnifications (× 4000 and × 10,000). The surface condition of each electrode was evaluated by an experienced investigator blinded to the experimental groups. Surface features, including mechanical damage, pitting corrosion, intergranular corrosion and surface deposits were evaluated. The severity of Pt corrosion was graded from 0 – 5 (0, no corrosion; 1, no evidence of corrosion but electrode partially coated with organic material; 2, localized minor corrosion; 3, localized moderate corrosion; 4, widespread corrosion; 5, severe and extensive corrosion) (8, 27, 28).

Representative unstained cochlear sections were examined under the SEM to identify particulate matter observed within the fibrous tissue capsule of some cochleae. Specific sites associated with the tissue capsule were selected for elemental analysis using an INCA X-Act SDD EDS system with an Oxford Aztec Microanalysis System (3.1). Regions of the fibrous tissue capsule containing the particulate material were compared with regions only containing fibrous tissue (8).

Trace analysis of platinum

The un-sectioned half of each cochlea was measured for Pt using ICP-MS by the National Measurement Institute of the Australian Government. Both the implanted and contralateral (control) cochleae were examined for trace Pt using this technique. Each tissue sample was washed and stored in de-ionised water. Because tissue samples were required to be > 0.5 g, cochlear tissue from each cohort were combined into a single analysis sample. Each sample was homogenized and digested in re-distilled nitric acid and hydrochloric acid (3:1) for 60 min in a DigiPrep block set (SCP Science) at 95°C and transferred to a Milestone microwave for 30 min to complete the digestion process. Liquid samples were micro filtered and analysed using an Agilent 7700X ICP-MS system. Pt trace analysis was reported as the mass of Pt per mass of tissue in each half cochlea (8).

Statistical analysis

Evoked potential and electrode impedance data were examined statistically by comparing the stimulated versus the unstimulated control cochleae using a 2 way repeated measures analysis of variance (RM ANOVA; electrode and time). Statistical comparisons of AN density were made by comparing each region of the stimulated cochlea with its unstimulated control cochlea (RM ANOVA; side and region). Finally, statistical comparison of the extent of fibrous tissue within the scala tympani and the degree of Pt electrode corrosion were performed using Kruskal-Wallis 1 way ANOVA (stimulated versus controls), with post hoc comparisons made using Dunn's method. Data are presented as mean and standard error of the mean (sem). An alpha level <0.05 was used to indicated significance for all tests.

Results:

3.1. Electrode impedance

Fifteen percent of the electrodes went open circuit as a result of leadwire breakage during the chronic stimulation program. This percentage was slightly higher than the implanted non-stimulated control animals (10% open circuit). The remaining functional electrodes exhibited a small, but significant increase in impedance from 12.2 ± 0.7 to 14.7 ± 1.2 kΩ over the course of the stimulation program ($p = 0.035$; Two way (Electrode, Time) RM ANOVA).

3.2. Electrically-evoked responses

EABRs were recorded and thresholds determined for each animal at implantation and on completion of the stimulation program in order to demonstrate the presence of functional ANs. There was no statistically significant difference in EABR threshold over the duration of the stimulation program for any cohort in the present study. There was, however, a small but significant increase in threshold from 184 ± 4 to 199 ± 6 CL over the duration of the stimulation program ($p = 0.043$; Two way (Electrode, Time) RM ANOVA) when all stimulated cohorts were combined.

3.3. Cochlear pathology

3.3.1. General cochlear pathology—There was evidence of electrode insertion trauma in less than 5% of the implanted cochleae in the present study. Because the trauma was localized and very minimal, no cochlea was withdrawn from the study; the tissue response was considered to be predominantly evoked by the chronically implanted electrode array and/or the electrical stimulation.

3.3.2 Tissue response—Figure 3 illustrates the typical tissue response observed in the UB turn adjacent to an electrode array for eight of the chronically implanted cohorts in the present study. Implanted, unstimulated control cochleae exhibited a minimal tissue response within the scala tympani (Fig. 3a). A mature fibrous tissue response was always evident in the UB turn of chronically stimulated cochleae. This typically took the form of a thin, mature tissue capsule surrounding the electrode array forming an electrode tract (ET; Fig. 3b), with loose mature fibrous tissue occupying much of the remainder of the scala tympani. A more extensive tissue response was evident at higher charge densities (compare Fig. 3b

with Fig. 3c–h). This response sometimes included a necrotic zone opposed to the electrode contact (e.g. Fig. 3e) and typically exhibited a zone of macrophages located around a section of the electrode tract (Fig. 3c–h). Under some stimulus conditions relatively large amounts of particulate material were evident in the tissue capsule (e.g. Fig. 3d & g). There was little evidence of a fibrous tissue response apical to the electrode array. Moreover, there were relatively small amounts of fibrous tissue adjacent to the unstimulated section of the electrode array in the LB turn. Finally, although a small number of cochleae exhibited neo-osteogenesis, there was no evidence of stimulus-induced new bone formation in any cochlea in this study.

The tissue response was quantified by measuring the total area of tissue occupying the scala tympani in the UB turn of each implanted cochlea (Fig. 4). There was a statistically significant increase in tissue response with charge density ($p = 0.007$, One-way ANOVA); with a post-hoc analysis specifically showing significant increases following stimulation at charge densities ≥ 200 $\mu C/cm^2$/phase compared to unstimulated cochleae ($p's < 0.012$, Holm-Sidak). There was no significant difference in the extent of the tissue response with charge recovery technique (i.e. electrode shorting alone versus electrode shorting with AP or CC; $p = 0.56$, One-way ANOVA).

In addition to an analysis of the total tissue response within the scala tympani, histological examination sometimes revealed focal regions of necrosis within the tissue capsule. These regions of necrosis consisted of amorphous acellular materials and were typically surrounded by a band of macrophages and plasma cells (Fig. 2). There was a statistically significant increase in the maximum thickness of the necrotic zone with charge density ($p = 0.032$, One-way ANOVA; Fig 5a).

A zone of macrophages were also observed between the electrode tract and the mature fibrous tissue response that occupied the majority of the scala tympani. There was a significant difference in the thickness of the macrophage zone with charge density ($p = 0.025$, One-way ANOVA, Fig. 5b). Finally, there was no significant difference in thickness of the necrotic and macrophage zones with charge recovery technique ($p = 0.54$ & $p = 0.35$ respectively; One-way ANOVA, Fig. 5a & b).

3.3.3 AN survival—Figure 6 illustrates the typical AN survival in the UB turn of both the left (adjacent to the stimulating electrodes) and the right (unimplanted control) cochleae for all cohorts in the present study. The relatively low packing density of ANs in the right control cochleae illustrate the typical degeneration of ANs observed following a sensorineural hearing loss. Compared to the close symmetry associated with AN survival in the implanted unstimulated control (Fig. 6a), the AN density in the UB region of the stimulated cochleae often exhibit greater AN survival than the contralateral control cochlea (e.g. Fig. 6b, e, g, h, i).

Figure 7 illustrates the mean AN density across cochlear region for both the implanted and contralateral control cochleae in this study. There was no stimulus induced reduction in AN density for any cohort. Indeed, AN survival showed a statistically significant increase in AN density in the UB turn (i.e. adjacent to chronically stimulated electrodes)

versus their contralateral control cochlea at charge densities of 100, 267, 267 CC, 400 and 540 CC μC/cm^2/phase ($p < 0.05$; Paired t-test; Fig. 7). The remaining cochlear turns typically showed close bilateral symmetry consistent with the highly symmetrical pattern of AN degeneration associated with systemic deafening. Finally, there was no statistically significant difference in AN survival with charge recovery technique ($p = 0.53$; One-way ANOVA).

3.4 Electrode corrosion

Scanning electron microscopy of the surface of electrodes was performed in order to evaluate the extent of corrosion across the cohorts and grade them on a scale from 0 (no corrosion) to 5 (extensive corrosion). In some cases, the Pt surface was covered with corrosion products and/or tissue that required removal prior to examination of the Pt surface. Representative micrographs from three electrodes on an array stimulated continuously for 4 weeks at 200 μC/cm^2/phase and 1000 pps (cohort 3) illustrate the range in Pt corrosion observed in the present study (Fig. 8). Electrode E1 served as an unstimulated control electrode; despite manufacturing marks on its surface, this electrode showed no evidence of corrosion (corrosion grade 0; Fig. 8a). Electrode E6 served as a flanker electrode and was therefore stimulated at ~ 100 μC/cm^2/phase. This electrode exhibited localised Pt corrosion (grade 2; Fig. 8b). Electrode E7 served as centre tripole and was stimulated at 200 μC/cm^2/phase. This electrode surface exhibited widespread corrosion (grade 4; Fig. 8c).

Representative SEM micrographs showing the effectiveness of CC in reducing corrosion on the Pt surface is illustrated in Fig. 9. The four electrodes were all centre tripole electrodes stimulated at 267 (Fig. 9a, b, c) or 540 μC/cm^2/phase (Fig. 9d) at 200 pps. Figure 9a illustrates the extensive corrosion observed following chronic stimulation at 267 μC/cm^2/phase using electrode shorting alone. In contrast, far less corrosion was apparent on the surface of electrodes stimulated at these high charge densities using electrode shorting with CC (Fig. 9c, d). Finally, the use of AP with electrode shorting reduced the level of corrosion compared with shorting alone, although not to the same extent as CC (Fig. 9b).

The SEM corrosion grading of all electrodes within each cohort were compared (Fig. 10). There was no significant difference across electrodes for both the implanted control (cohort 1; $p = 0.84$; $n = 4$) and 100 μC/cm^2/phase cohorts (cohort 2; $p = 0.60$; $n = 5$ ANOVA by Ranks). Corrosion grades for these two cohorts varied between 0 (no corrosion) and 1 (no corrosion although evidence of a coating over part of the electrode surface). In contrast, there were statistically significant differences in corrosion grading across electrodes in all other cohorts. Electrodes E4 and E7 (centre tripole electrodes) in all these cohorts exhibited significantly greater corrosion grades compared to unstimulated electrodes ($p < 0.05$; Dunn's post hoc analysis), while both flanker electrodes (E3, E5, E6 and E8) and centre tripole electrodes exhibited significantly greater levels of corrosion compared with control electrodes E1 and E2 in cohorts 3 – 6 & 8 ($p < 0.05$; Dunn's post hoc analysis). Finally, in the cohorts that exhibited the most extensive corrosion grades (cohorts 5, 6 & 8), the level of corrosion for the centre tripole electrodes were also significantly greater than their flanker electrodes ($p < 0.05$; Dunn's post hoc analysis).

3.5 Analysis of particulate deposits

There was clear evidence of particulate deposits in all cochleae stimulated at charge densities ≥ 200 μC/cm^2/phase using electrode shorting alone (cohorts 3–5, 8; e.g. Fig. 11). Particulate matter was apparent in the electrode-tissue capsule of the UB turn proximal to the chronically stimulated tripolar electrodes centred on electrode E7. This material was typically localized close to the electrode tract. There was minimal evidence of particulate deposits in the tissue capsule associated with any cochlea stimulated at 267 or 540 μC/cm^2/phase that combined electrode shorting with CC (cohorts 7 & 9), and only minor particulate material in one cochlea stimulated at 267 μC/cm^2/phase in the AP cohort (cohort 6).

The majority of the material appeared to be of sub-micron dimensions and readily phagocytosed by macrophages, while there were occasional larger deposits (~ 20 μm in length) that had not undergone phagocytosis (Fig. 11). This particulate material was identified as Pt using SEM-EDS (data not illustrated).

Each cochlea was examined histologically for the presence of particulate Pt and qualitatively graded from 0 (no material present) to 4 (widespread particulate material present). Figure 12 illustrates the extent of Pt corrosion products within the scala tympani as a function of charge density. There was a difference in the amount of particulate Pt with both charge density ($p < 0.01$; One way ANOVA) and the charge recovery technique ($p < 0.01$; One way ANOVA, Fig. 12). Reduced levels of Pt corrosion product were evident in animals stimulated using AP or CC charge recovery techniques.

3.6 Trace analysis of platinum

ICP-MS analysis did not detect Pt in the unimplanted contralateral cochleae at the detection limit of the spectrometer (0.01 mg/kg). In contrast, trace levels were present in all implanted cochleae including just detectable levels in the implanted, unstimulated control cochleae (Table 2). The level of Pt was dependent on the charge density and appeared to be also influenced by the charge recovery technique; reduced levels were associated with CC and, to a less extent, with AP.

Discussion:

We evaluated the quantity of Pt corrosion using three measures: (i) the amount of Pt corrosion product observed in cochlear histology; (ii) the extent of Pt corrosion associated with the surface of the electrodes examined under SEM; and (iii) trace analysis of Pt in cochleae measured using ICP-MS. These three techniques showed consistent findings: the level of Pt corrosion increased with charge density and was reduced in cohorts stimulated using electrode shorting with CC or AP. Consistent with our previous report (8), the extent of the tissue response within cochleae was dependent on charge density; all cochleae stimulated at ≥ 200 μC/cm^2/phase exhibited a vigorous tissue response localized to the site of stimulation, and stimulation at high charge densities resulted in a focal region of necrosis and a zone of macrophages close to the Pt electrode. Notably, the extent of the tissue response was not affected by the charge recovery technique, implying that tissue response is not influenced by the amount of particulate Pt within the cochlea. Finally, despite chronic

stimulation at intense change densities as high as 540 μC/cm^2/phase producing a vigorous tissue response and Pt corrosion products, there was no evidence of stimulus induced neural loss or loss of neural function.

Pt dissolution and charge recovery

CC and AP have been shown to eliminate or reduce DC leakage current respectively (13, 15); it is therefore tempting to speculate that at least part of the process underlying Pt dissolution is associated with DC. Previous data linking DC and dissolution in neural stimulators is, however, conflicting. Most of the historical work, both *in vivo* and *in vitro*, used CC devices (e.g. (11, 12, 29)). In these cases the DC was zero and yet significant rates of dissolution were reported, suggesting a mechanism unrelated to DC. Moreover, unpublished stimulation experiments in physiological saline by one of the authors (PMC) found little difference between dissolution rates with and without CC. On the other hand, if a constant potential is applied to an electrode in solution, the level of dissolution reduces initially (30) and then stabilises to a level that is a strong function of the level of DC (31). Clearly DC and dissolution are related in this instance.

Our findings echo the dichotomy observed in the literature. In support of a mechanism unrelated to DC, animals in cohort 3 in the present study were stimulated at significantly higher rates than other cohorts (1000 versus 200 pps). Higher stimulus rates are associated with elevated DC leakage current using electrode shorting (13), however there was no marked difference in either the degree of electrode corrosion or particulate Pt within the cochleae of this cohort compared with other groups stimulated at high charge densities. Conversely, the modest reduction in dissolution due to AP (cohort 6) compared to the same phase equivalent (cohort 5), provides an argument for a DC-related mechanism. The effect of AP stimulation is to reduce DC *and* increase the potential range over which the electrode interface transitions. Had the potential range increased (for example, by delivering more charge) without the associated reduction in DC, this would likely have increased dissolution, suggesting dissolution is dependent on the DC level.

One solution to these apparent discrepancies is to propose two mechanisms that contribute to Pt dissolution; one dependent on DC and one not. A good candidate for the DC-independent mechanism is one described by Topalov and colleagues (32), where dissolution occurs due to voltage transitions of the Pt/electrolyte interface through the oxide formation and reduction regions. These transitions occur during the delivery of every stimulus pulse whether or not a coupling capacitor is present. For the DC-dependent findings, the (anodic) oxygen evolution reaction of Pt ($2OH^- \Rightarrow H_2O + ½O_2 + 2e^-$) is known to promote dissolution (33) and may be the mechanism responsible at anodic potentials. Oxygen evolution is, however, an anodic process and cannot easily explain the dissolution that occurred at the cathodic-first centre electrodes of our tripoles. Also, the passage of cathodic DC has been shown to produce more dissolution than anodic DC (31). A cathodic Pt dissolution mechanism has been described caused by the reduction of molecular oxygen in solution: oxygen is reduced at the cathode to H_2O_2 ($O_2 + 2H^+ + 2e^- \Rightarrow H_2O_2$) which is then further reduced to the highly oxidising hydroxyl radical OH^0 ($H_2O_2 + e^- \Rightarrow OH^- + OH^0$). Although not fully understood, it is thought this short-live radical may be responsible for

Pt dissolution through the oxidation of Pt metal to its ionic form ($2OH^0 + 2Pt => 2Pt^{2+} + 2OH^-$) (34, 35).

The use of CC forces zero DC to flow through an electrode, which in turn forces the total anodic and total cathodic by-products at the electrode to be equal. It does not, as is sometimes thought, eliminate irreversible by-products at the electrode altogether. To achieve this anodic/cathodic balance, CC forces the electrode to change its potential, through the mechanism of slideback (3, 36), to a position that minimises irreversible by-products. This complex set of actions resulting from CC reduces dissolution *in vivo* compared with AP and shorting alone. However, dissolution can still occur at significant levels with CC. For example, CC stimulation at the highest charge density used in the present study (540 $\mu C/cm^2$/phase; cohort 9), resulted in higher levels of Pt in tissue, when normalised for electrode area, than cohort 5 which used half the charge density and electrode shorting. Whether dissolution during CC stimulation predominantly occurs due to the potential transition mechanism (32), an equal combination of irreversible oxidation and reduction reactions (e.g. oxygen evolution during the anodic phase and oxygen reduction during the cathodic phase), or some other mechanism is unclear. Our observations are, however, consistent with other data describing the presence of particulate Pt in all cochlear specimens examined from long-term implant users (7). These devices used a variety of charge recovery techniques including electrode shorting alone and electrode shorting with CC.

The origin of the particulate Pt is unclear. It seems unlikely to result directly from flaking of electrode material as manufactured since all electrode arrays underwent an extensive cleaning program prior to implantation that included sonication, and the unstimulated electrodes surfaces were in general quite smooth (Fig. 1). In addition, the nature of the particulate Pt observed histologically were sub-micron in size, with the significant majority of particles phagocytosed; Pt fragments produced during manufacture are likely to be considerably larger. Platinum and other metals can undergo a surface flaking process known as spalling when electrodes are pulsed repeatedly under certain conditions. The upper and lower potentials reached by the electrode when being pulsed are critical to this process (36). As noted above, the addition of AP or CC to shorting will modify these potentials and may explain the large difference in particulate scores between shorting, AP and CC, while the trace levels of Pt in tissue show far less variation. Another possibility is that the Pt particles form through reduction of ionic Pt, perhaps due to conditions generated at the cellular level which favour reduction (e.g. $PtCl_4^{2-} + 2e^- -> Pt^0 + 4Cl^-$). Such a process may occur when Pt ions are above a certain concentration in tissue.

As we have previously reported (8), the particulate Pt observed histologically was localized within the tissue capsule proximal to the electrode tract, and the majority of the Pt was phagocytosed by macrophages although some larger deposits were not. There was little evidence of this particulate material distal to the electrode-tissue capsule. For example, no particulate material was observed in Rosenthal's canal, the scala media, or scala vestibuli.

While the present study demonstrated that Pt dissolution *in vivo* is related to charge density, it does not provide insight into the rate of Pt dissolution over time. A number of previous *in vivo* studies have shown that there is a rapid increase Pt corrosion product following

the onset of stimulation (37), and the rate of this dissolution gradually decreases during stimulation (38).

The three measures of Pt corrosion used in the present study were complementary and each had a specific methodological strength. Trace analysis using ICP-MS provided a highly sensitive quantitative measure of Pt dissolution, while SEM examination of the electrode surface provided a qualitative measure of corrosion for each electrode on the array that could be related to its specific stimulation history (i.e. centre tripole; flanker or control electrode). Finally, the evaluation of particulate Pt within cochlear histology provided a quantitative estimate of Pt across cohorts as well as insight into the cellular response and the location of the particulate in relation to the electrode-tissue interface.

Although these three methods of evaluating Pt dissolution were in broad agreement, there were some disparities between techniques, presumably as a result of the semi-quantitative assessment method used for the particulate Pt assessment. Specifically, the mean score for particulate Pt observed histologically in implanted unstimulated controls (cohort 1) was ~1 (Fig. 12) while the corresponding trace analysis for Pt was 1 ng/mg/half cochlea (Table 2). In contrast, particulate Pt scores for cochleae stimulated using CC and shorting (cohorts 7 and 9) were between 0 and 1 (Fig. 12) with corresponding trace Pt levels of 61 and 93 ng/mg/half cochleae (Table 2). We attribute this discrepancy to the grading method associated with the particulate Pt scoring, in particular the potential for lack of precision when assessing levels 0 (no evidence of particulate material in any section) and 1 (possible particulate material present).

Finally, there were detectable levels of Pt in the implanted, unstimulated control cochleae (cohort 1), albeit approximately two orders of magnitude less than the levels observed in stimulated cochleae. While it is possible that this level of Pt may be associated with small fragments of the metal flaking off the electrode surface, we cannot dismiss the possibility that Pt electrodes undergo small amounts of corrosion *in vivo* in the absence of stimulation. Longer-term studies evaluating Pt corrosion in implanted control cochleae are warranted.

Tissue response and Pt dissolution

The tissue response in the present study was in the form of a mature foreign body response that included a compact tissue capsule around the array, and loose vascularized fibrous tissue occupying much of the remainder of the scala tympani proximal to the electrode array. These findings are consistent with previous studies examining the inflammatory response associated with cochlear implantation (39, 40). In addition to this mature tissue response, histological examination of cochleae stimulated at levels ≥ 267 $\mu C/cm^2$/phase exhibited focal regions of necrosis associated with the tissue capsule consisting of amorphous acellular material typically surrounded by a band of macrophages and plasma cells. The location and dimensions of these focal necrotic zones were consistent with the size of the Pt electrode contact and are likely to be associated with the presence of local toxic by-products associated with these high charge densities.

The present findings support our previous observations showing a clear relationship between electrical stimulation at moderate to high charge densities and a vigorous tissue response

restricted to the region proximal to the electrode array (8). In cochlear regions apical to the array there was minimal evidence of a tissue response. These results are also consistent with clinical findings reporting that the formation of a robust fibrous tissue sheath proximal to the site of electric stimulation (41).

As noted above, we described regions of focal necrosis proximal to the stimulating electrodes. This localized tissue response had features similar to those described by Agnew and colleagues (37). Although all implanted cochleae examined in the present study contained trace levels of Pt, our results indicate that the necrotic response was unrelated to the presence of Pt corrosion product observed histologically.

Relationship to the defined safety limits for Pt electrodes

Cochlear implants voluntarily conform to the Association for the Advancement of Medical Instrumentation standard for commercial cochlear implants (23). This standard defines the Shannon limit ($k = 1.75$) and also imposes a maximum charge density of 216 $\mu C/cm^2$/phase as the safe stimulation limit for these devices (23). The present study included stimulus parameters well above this standard, achieving $k = 2.0$ for the highest charge density (540 $\mu C/cm^2$/phase); a value 77% greater in terms of charge density than the AAMI limit, and more than 300% greater than Shannon's proposed 'conservative' limit of $k = 1.5$ (42).

While these stimulus levels were not damaging to ANs or the cochlea in general, the detection of trace levels of Pt and evidence of Pt corrosion associated with electrodes stimulated at levels less than 216 $\mu C/cm^2$/phase, suggest that Pt dissolution would occur within this limit. It should be noted, however, that typical clinical levels of cochlear implant stimulation are approximately an order of magnitude lower than the recommended AAMI limit.

Status of Auditory Neurons

There was no evidence of a stimulus-induced reduction in AN survival in any cohort in the present study, despite stimulation at high charge densities and the presence of significant levels of Pt corrosion products. Indeed, in contrast to contralateral control cochleae, there was a statistically significant increase in AN survival proximal to the site of stimulation in a number of cohorts including those stimulated at the highest charge densities. Although not consistently observed across cohorts, the results indicate the possibility of a stimulus-induced rescue effect of ANs in response to the normal pattern of degeneration that occurs following hearing loss (43). Similar effects have been reported previously (44).

The functional status of ANs was monitored by measuring the change in EABR threshold recorded prior to and on completion of the 28 day stimulation program. There was no significant increase in EABR threshold for any stimulated cohort in the present study. These data support the conclusion that stimulation over the range of charge densities used in the present study did not adversely affect ANs.

Electrode impedance, electrode surface area, and Pt corrosion

We observed a small but statistically significant overall increase in impedance over the 28 day stimulation period. While pitting corrosion, observed on centre tripole electrodes stimulated at ≥ 200 μC/cm^2/phase, would produce an increase in the real surface area of the electrode, it is likely that any resultant reduction in impedance would be nullified by the presence of a more extensive fibrous tissue response. Given these competing factors – a simultaneous increase in both real surface area and tissue response – more detailed impedance monitoring, such as electrochemical impedance spectroscopy, may provide greater insight into the electrical properties of both the electrode and the tissue interface (9, 45).

The present study used charge densities over an order of magnitude larger than clinical levels in order to provoke and accelerate Pt dissolution mechanisms. Despite the extent of Pt dissolution reported here, accumulated Pt corrosion products do not appear to be associated with any untoward effects on the cochlea. The extent of Pt dissolution would not apply to devices in clinical use because of the large difference in charge densities. However, the development of smaller electrode contacts using thin Pt films reduces the likely dissolution life of an electrode. *In vivo* studies examining the dissolution rates of thin film Pt electrodes considered for clinical application should be undertaken in order to compare with that of bulk Pt electrodes (46).

Clinical implications

Studies involving the histological examination of cochleae taken from patients that were long-term cochlear implant users describe particulate Pt within the tissue capsule surrounding the electrode array (4–7). In one study, particulate Pt was observed in all 45 cochlear specimens examined; the study included a variety of commercial devices (7), implying that Pt corrosion product is relatively common in cochleae of long-term cochlear implant users. Despite the important clinical implications, little is known about the long-term effects of Pt within the body, although the present study and our previous research (8) suggests that there are no untoward effects associated with Pt within the cochlea.

Clinically, the major source of systemic Pt is associated with the use of Pt-based chemotherapy drugs such as Cisplatin (47, 48). Typically administered intravenously, Pt accumulates in the kidney, liver and spleen (48). At high doses Cisplatin is nephrotoxic, although this is thought to be associated with the cellular mechanisms associated with its effect on tumours rather that the toxicity of Pt *per se* (47).

Longer-term *in vivo* studies are required to corroborate the present findings that stimulus-induced Pt corrosion does not adversely affect ANs or the cochlea in general. Moreover, although all Pt deposits in the present study appeared to be localized to the electrode-tissue interface, there is no data on whether Pt accumulation occurs in other organs. This work is currently under investigation in our laboratory.

Finally, although there appears to be less evaluation of post-mortem tissue from patients implanted with other neural prostheses, it is reasonable to expect, based on clinical data associated with cochlear implants, that Pt corrosion products will be present in these

tissues. For example, there are reports of electron dense particulate material obtained from tissue samples of DBS patients (49, 50). One study described multinucleated giant cells and macrophages with highly electron-dense inclusions thought to represent phagocytosed material at the electrode-tissue interface (50). While the authors did not identify the nature and origin of the material, it is likely to be Pt corrosion product from the DBS electrodes. Examination of post-mortem tissue from long-term neuroprosthesis users to evaluate the presence and extent of Pt corrosion products and tissue response is recommended.

Conclusions

Long-term intracochlear stimulation at intense charge densities of up to 540 $\mu C/cm^2$/phase showed that Pt corrosion product was dependent on charge density. The level of corrosion reduced with the use of charge recovery techniques including electrode shorting with capacitive coupling and, to a lesser extent, electrode shorting with alternating leading phase. It would appear it is not possible to completely eliminate Pt accumulation as trace levels were also detected in implanted, unstimulated cochleae. The tissue response, which included localized necrotic and macrophage sites proximal to the electrode contact, and a mature fibrous tissue response within the scala tympani, were also charge density dependent. However, the amount of Pt corrosion product did not influence the tissue response. Finally, the presence of Pt corrosion product and/or chronic stimulation at high charge densities did not adversely affect the ANs.

Acknowledgements:

This work was supported by NIDCD (R01DC015031) and Cochlear Ltd. The Bionics Institute acknowledges support of the Victorian Government through Operational Infrastructure Support Program. We thank C. Singleton, C. McGowan, H. Feng, J. Zhou, N. Critch, Dr T. Nguyen, C. Grenness, C. Sloan, D. Tuari, S. Barone and J. Firth from the Bionics Institute, R. Curtain from the SEM Facility at Bio21, University of Melbourne for their excellent technical assistance, A/Prof A. Wise for histological advice, the staff at the National Measurement Institute of the Australian Government for ICP-MS analysis and Prof Richard Williams, Pathology Department, St Vincent's Hospital, Melbourne for histopathology advice.

References:

1. Shepherd RK, Villalobos J, Burns O, Nayagam DAX. The development of neural stimulators: a review of preclinical safety and efficacy studies. J Neural Eng. 2018;15(4):041004. [PubMed: 29756600]
2. Cogan SF, Ludwig KA, Welle CG, Takmakov P. Tissue damage thresholds during therapeutic electrical stimulation. J Neural Eng. 2016;13(2):021001. [PubMed: 26792176]
3. Merrill DR, Bikson M, Jefferys JG. Electrical stimulation of excitable tissue: design of efficacious and safe protocols. J Neurosci Methods. 2005;141(2):171–98. [PubMed: 15661300]
4. Clark GM, Clark J, Cardamone T, Clarke M, Nielsen P, Jones R, et al. Biomedical studies on temporal bones of the first multi-channel cochlear implant patient at the university of Melbourne. Cochlear Implants Int. 2014.
5. Spiers K, Cardamone T, Furness JB, Clark JCM, Patrick JF, Clark GM. An X-ray fluorescence microscopic analysis of the tissue surrounding the multi-channel cochlear implant electrode array. Cochlear Implants Int. 2016;17(3):129–31. [PubMed: 27078517]
6. Nadol JB Jr., O'Malley JT, Burgess BJ, Galler D. Cellular immunologic responses to cochlear implantation in the human. Hear Res. 2014;318:11–7. [PubMed: 25285622]
7. O'Malley JT, Burgess BJ, Galler D, Nadol JB Jr,. Foreign Body Response to Silicone in Cochlear Implant Electrodes in the Human. Otology & neurotology. 2017;38(7):970–7. [PubMed: 28538471]

8. Shepherd RK, Carter P, Enke YL, Wise AK, Fallon JB. Chronic intracochlear electrical stimulation at high charge densities results in platinum dissolution but not neural loss or functional changes in vivo. J Neural Eng. 2019;16:026009. [PubMed: 30523828]
9. Cogan SF. Neural stimulation and recording electrodes. Annu Rev Biomed Eng. 2008;10:275–309. [PubMed: 18429704]
10. Shepherd RK, Fallon JB, McDermott H. Medical Bionics. In: Brahme A, editor. Comprehensive Biomedical Physics. 10. Amsterdam: Elsevier; 2014. p. 327–41.
11. Brummer SB, Turner MJ. Electrochemical considerations for safe electrical stimulation of the nervous system with platinum electrodes. IEEE Trans Biomed Eng. 1977;24(1):59–63. [PubMed: 851475]
12. Robblee LS, Rose TL. Electrochemical guidelines for selection of protocols and electrode materials for neural stimulation. In: Agnew WF, McCreery DB, editors. Neural Prostheses - Fundamental Studies. Englewood Cliffs, New Jersey: Prentice Hall; 1990. p. 25–66.
13. Huang CQ, Shepherd RK, Carter PM, Seligman PM, Tabor B. Electrical stimulation of the auditory nerve: direct current measurement in vivo. IEEE Trans Biomed Eng. 1999;46(4):461–70. [PubMed: 10217884]
14. Agnew WF, Yuen TG, Pudenz RH, Bullara LA. Electrical stimulation of the brain. IV. Ultrastructural studies. Surg Neurol. 1975;4(5):438–48. [PubMed: 171783]
15. Huang CQ, Carter PM, Shepherd RK. Stimulus induced pH changes in cochlear implants: an in vitro and in vivo study. Ann Biomed Eng. 2001;29(9):791–802. [PubMed: 11599587]
16. Swiontek T, Maiman D, Sances A Jr., Myklebust J, Larson S, Hemmy D. Effect of electrical current on temperature and pH in cerebellum and spinal cord. Surg Neurol. 1980;14(5):365–9. [PubMed: 7444745]
17. Shepherd RK, Linahan N, Xu J, Clark GM, Araki S. Chronic electrical stimulation of the auditory nerve using non-charge- balanced stimuli. Acta Otolaryngol. 1999;119(6):674–84. [PubMed: 10587001]
18. Patrick JF, SeIigman PM, Money DK, Kuzma JA. Engineering. In: Clark GM, Tong YC, Patrick JF, editors. Cochlear Prostheses. Edinburgh: Churchill Livingston; 1990. p. 99–124.
19. Landry TG, Fallon JB, Wise AK, Shepherd RK. Chronic neurotrophin delivery promotes ectopic neurite growth from the spiral ganglion of deafened cochleae without compromising the spatial selectivity of cochlear implants. J Comp Neurol. 2013;521(12):2818–32. [PubMed: 23436344]
20. Xu J, Shepherd RK, Millard RE, Clark GM. Chronic electrical stimulation of the auditory nerve at high stimulus rates: a physiological and histopathological study. Hear Res. 1997;105:1–29. [PubMed: 9083801]
21. Shepherd RK, Coco A, Epp SB, Crook JM. Chronic depolarization enhances the trophic effects of brain-derived neurotrophic factor in rescuing auditory neurons following a sensorineural hearing loss. J Comp Neurol. 2005;486(2):145–58. [PubMed: 15844207]
22. Senn P Neurostimulation for the management of pain. [PhD]. Melbourne: University of Melbourne; 2015.
23. ANSI. Cochlear Implant Systems: Requirements for safety, functional verification, labeling and reliability reporting. ANSI/AAMI CI86:2017. Arlington, VA: AAMI; 2017. p. 169.
24. Wise AK, Tan J, Wang Y, Caruso F, Shepherd RK. Improved Auditory Nerve Survival with Nanoengineered Supraparticles for Neurotrophin Delivery into the Deafened Cochlea. PLoS One. 2016;11(10):e0164867. [PubMed: 27788219]
25. Xu J, Shepherd RK, Millard RE, Clark GM. Chronic electrical stimulation of the auditory nerve at high stimulus rates: a physiological and histopathological study. Hear Res. 1997;105(1–2):1–29. [PubMed: 9083801]
26. Leake-Jones PA, Rebscher SJ. Cochlear pathology with chronically implanted scala tympani electrodes. Ann N Y Acad Sci. 1983;405:203–23. [PubMed: 6575646]
27. Shepherd RK, Wise AK, Enke YL, Carter PM, Fallon JB. Evaluation of focused multipolar stimulation for cochlear implants: a preclinical safety study. J Neural Eng. 2017;14(4):046020. [PubMed: 28607224]
28. Dalrymple AN, Huynh M, Robles UA, Marroquin JB, Lee CD, Petrossians A, et al. Electrochemical and mechanical performance of reduced graphene oxide, conductive hydrogel,

and electrodeposited Pt-Ir coated electrodes: an active in vitro study. J Neural Eng. 2019;17(1):016015. [PubMed: 31652427]

29. McHardy J, Robblee LS, Marston JM, Brummer SB. Electrical stimulation with pt electrodes. IV. Factors influencing Pt dissolution in inorganic saline. Biomaterials. 1980;1(3):129–34. [PubMed: 7470563]
30. Topalov AA, I. K, Auinger M, Cherevko S, Meier JC, Klemm SO, et al. Dissolution of Platinum: Limits for the Deployment of Electrochemical Energy Conversion Angew Chem Int Ed 2012;51:12613–5.
31. Black RC, Hannaker P. Dissolution of smooth platinum electrodes in biological fluids. Appl Neurophysiol. 1980;42(6):366–74. [PubMed: 6966483]
32. Topalov AA, Cherevko S, Zeradjanin AR, Meier JC, Katsounaros I, Mayrhofer KJJ. Towards a comprehensive understanding of platinum dissolution in acidic media. Chem Soc. 2014;5:631–8.
33. Cherevko S, Zeradjanin AR, Topalov AA, Kulyk N, Katsounaros I, Mayrhofer KJJ. Dissolution of Noble Metals during Oxygen Evolution in Acidic Media. Chem Cat Chem. 2014;6(8):2219–23.
34. Percival SJ, Dick JE, Bard AJ. Cathodically Dissolved Platinum Resulting from the O-2 and H2O2 Reduction Reactions on Platinum Ultramicroelectrodes. Anal Chem. 2017;89(5):3087–92. [PubMed: 28194948]
35. Noel J-M, Yu Y, Mirkin MV. Dissolution of Pt at Moderately Negative Potentials during Oxygen Reduction in Water and Organic Media. Langmuir. 2013;29(5):1346–50. [PubMed: 23323756]
36. Donaldson NN, Donaldson PE. Performance of platinum stimulating electrodes mapped on the limit-voltage plane. Part 2. Corrosion in vitro. Med Biol Eng Comput. 1986;24(4):431–8. [PubMed: 3491939]
37. Agnew WF, Yuen TG, McCreery DB, Bullara LA. Histopathologic evaluation of prolonged intracortical electrical stimulation. Exp Neurol. 1986;92(1):162–85. [PubMed: 3956647]
38. Robblee LS, McHardy J, Agnew WF, Bullara LA. Electrical stimulation with Pt electrodes. VII. Dissolution of Pt electrodes during electrical stimulation of the cat cerebral cortex. J Neurosci Methods. 1983;9(4):301–8. [PubMed: 6668956]
39. Foggia MJ, Quevedo RV, Hansen MR. Intracochlear fibrosis and the foreign body response to cochlear implant biomaterials. Laryngoscope Investig Otolaryngol. 2019;4(6):678–83.
40. Bas E, Goncalves S, Adams M, Dinh CT, Bas JM, Van De Water TR, et al. Spiral ganglion cells and macrophages initiate neuro-inflammation and scarring following cochlear implantation. Front Cell Neurosci. 2015;9:303. [PubMed: 26321909]
41. Ishai R, Herrmann BS, Nadol JB Jr., Quesnel AM. The pattern and degree of capsular fibrous sheaths surrounding cochlear electrode arrays. Hear Res. 2017;348:44–53. [PubMed: 28216124]
42. Shannon RV. A model of safe levels for electrical stimulation. IEEE Trans Biomed Eng. 1992;39(4):424–6. [PubMed: 1592409]
43. Wise AK, Pujol R, Landry TG, Fallon JB, Shepherd RK. Structural and Ultrastructural Changes to Type I Spiral Ganglion Neurons and Schwann Cells in the Deafened Guinea Pig Cochlea. J Assoc Res Otolaryngol. 2017.
44. Leake PA, Snyder RL, Hradek GT, Rebscher SJ. Consequences of chronic extracochlear electrical stimulation in neonatally deafened cats. Hear Res. 1995;82:65–80. [PubMed: 7744715]
45. Dalrymple AN, Robles UA, Huynh M, Nayagam BA, Green RA, Poole-Warren LA, et al. Electrochemical and biological performance of chronically stimulated conductive hydrogel electrodes. J Neural Eng. 2020;17(2):026018. [PubMed: 32135529]
46. Dalrymple AN, Huynh M, Nayagam BA, Lee C, Weiland GR, Petrossians A, et al. Electrochemical and biological characterization of thin-film platinum-iridium alloy electrode coatings: a chronic in vivo study. J Neural Eng. 2020.
47. Miller RP, Tadagavadi RK, Ramesh G, Reeves WB. Mechanisms of Cisplatin nephrotoxicity. Toxins (Basel). 2010;2(11):2490–518. [PubMed: 22069563]
48. Madias NE, Harrington JT. Platinum nephrotoxicity. Am J Med. 1978;65(2):307–14. [PubMed: 99034]
49. Haberler C, Alesch F, Mazal PR, Pilz P, Jellinger K, Pinter MM, et al. No tissue damage by chronic deep brain stimulation in Parkinson's disease. Ann Neurol. 2000;48(3):372–6. [PubMed: 10976644]

50. Moss J, Ryder T, Aziz TZ, Graeber MB, Bain PG. Electron microscopy of tissue adherent to explanted electrodes in dystonia and Parkinson's disease. Brain. 2004;127(Pt 12):2755–63. [PubMed: 15329356]

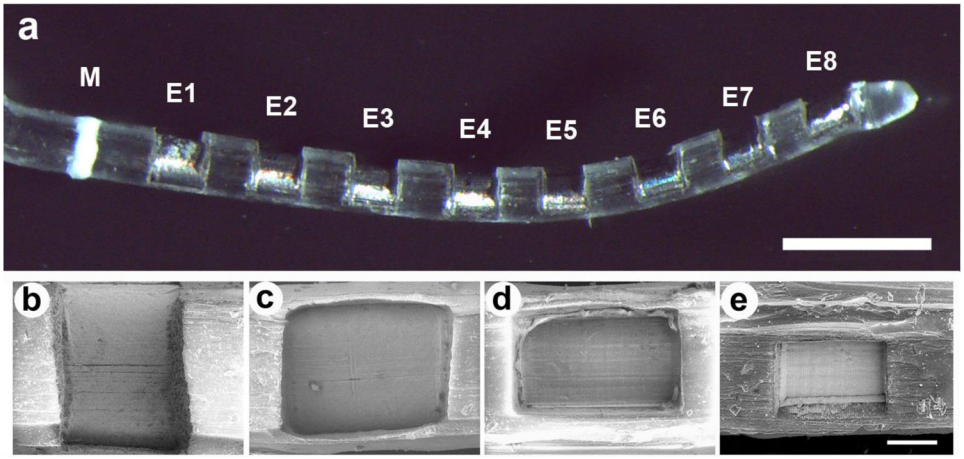

Figure 1.

(a) Low power micrograph of an HL8 electrode array illustrating the 8 Pt electrodes (E1–E8) on a PDMS silicone carrier. All Pt contact areas on each array were identical. The white band (M) was used as a surgical guide to ensure a uniform insertion depth for each electrode array. Scale bar = 1 mm. (b) – (e) Scanning electron micrographs illustrating four of the six Pt contact areas used in this study; (b) 0.2 mm^2; (c) 0.085 mm^2; (d) 0.075 mm^2; and (e) 0.0375 mm^2. Scale bar = 100 μm.

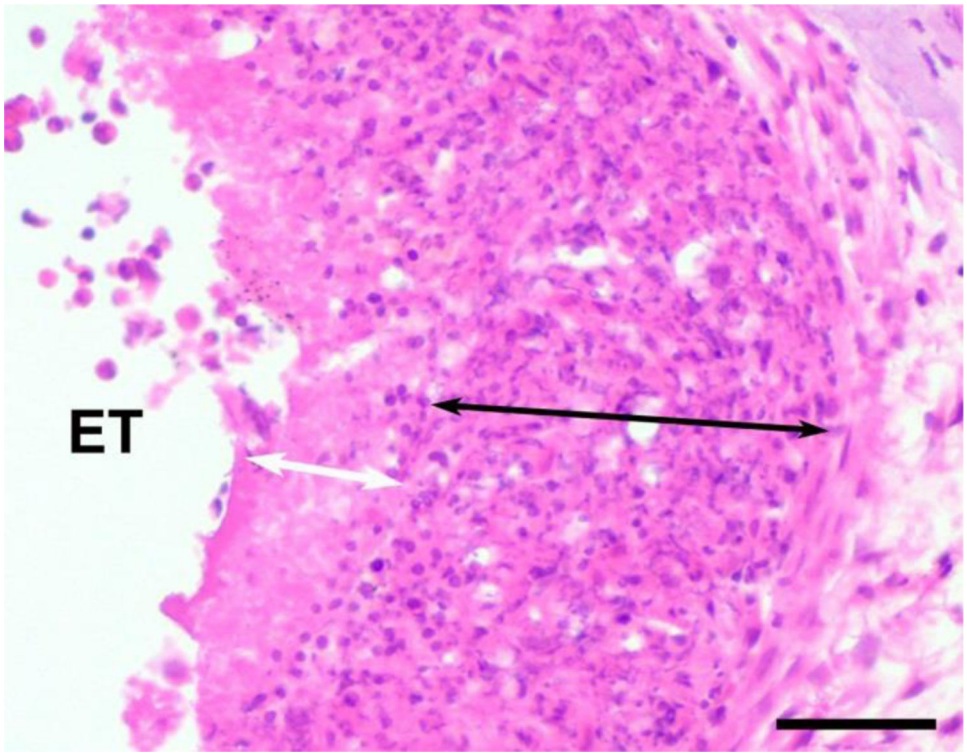

Figure 2.

Example illustrating the technique used to measure the width of the necrotic zone containing only cellular debris (white arrow), and the macrophage zone (black arrow). A necrotic zone was only occasionally observed, while a macrophage zone was commonly observed and located between the electrode array and loose fibrous tissue which typically occupied the remainder of the scala tympani. ET = electrode tract. Scale bar = 50 μm.

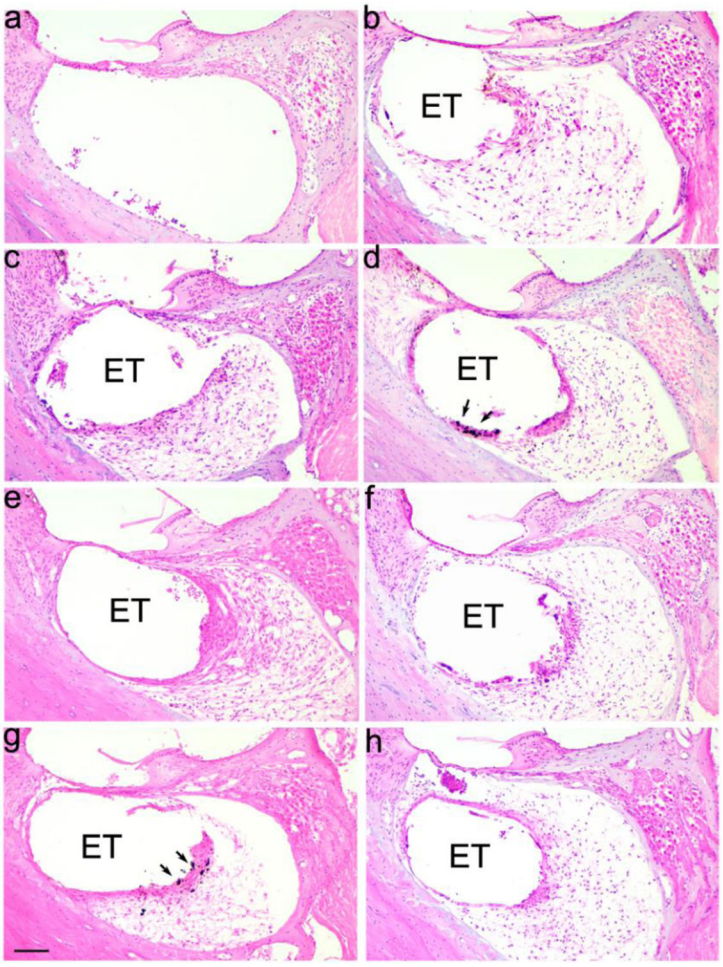

Figure 3.

Representative micrographs illustrating tissue response within the UB turn of the scala tympani. (a) Implanted unstimulated cochleae. (b)-(h) All stimulated cochleae exhibited a clear tissue response with the most extensive response evident in cochleae stimulated at charge densities ≥ 200 μC/cm^2/phase; (b) 100; (c) 228, (d) 267; (e) 267 AP; (f) 267 CC; (g) 400 and (h) 540 CC μC/cm^2/phase. ET = electrode tract. Arrows illustrate examples of particulate material within the tissue capsule. Scale bar = 100 μm.

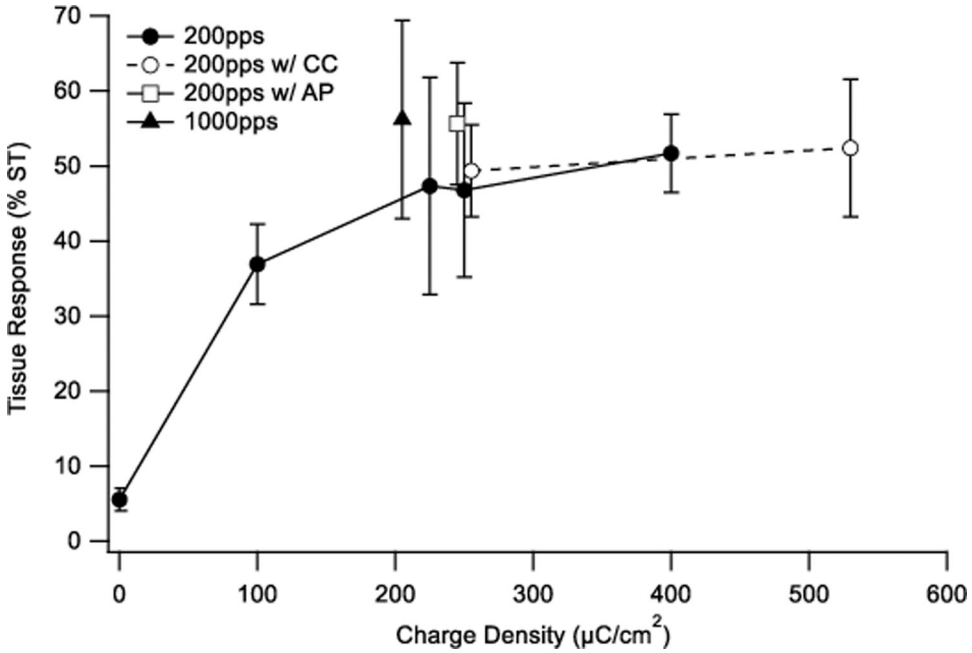

Figure 4.

Mean extent of tissue response expressed as a percentage of the area of the scala tympani, occupying the UB turn scala tympani in the nine chronically implanted cohorts in this study. There was a statistically significant difference in fibrous tissue response associated with charge density ($p = 0.007$); however, the tissue response was independent of the charge recovery technique ($p=0.56$). Error bars = sem.

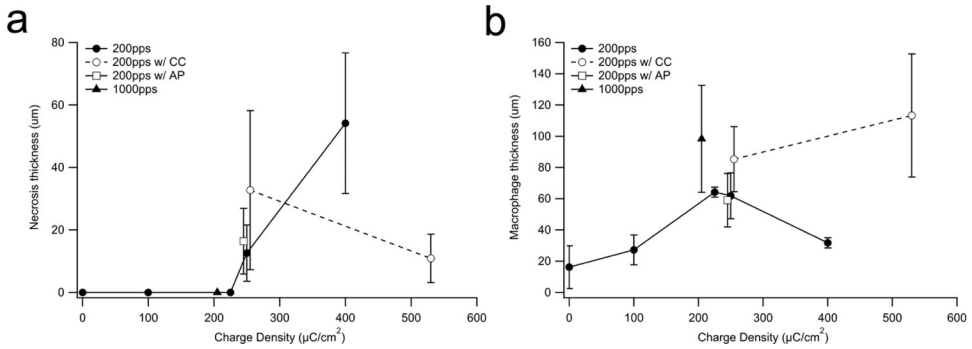

Figure 5.

(a) Mean thickness of the necrotic zone versus charge density within the UB turn. Necrosis was only observed in cochleae stimulated at charge densities ≥ 267 μC/cm^2/phase. The extent of the necrotic zone was not associated with the charge recovery technique ($p = 0.54$). (b) Mean thickness of the macrophage zone within the UB turn usually increased with charge density. This response was independent of the charge recovery technique used ($p = 0.35$). Error bar = sem.

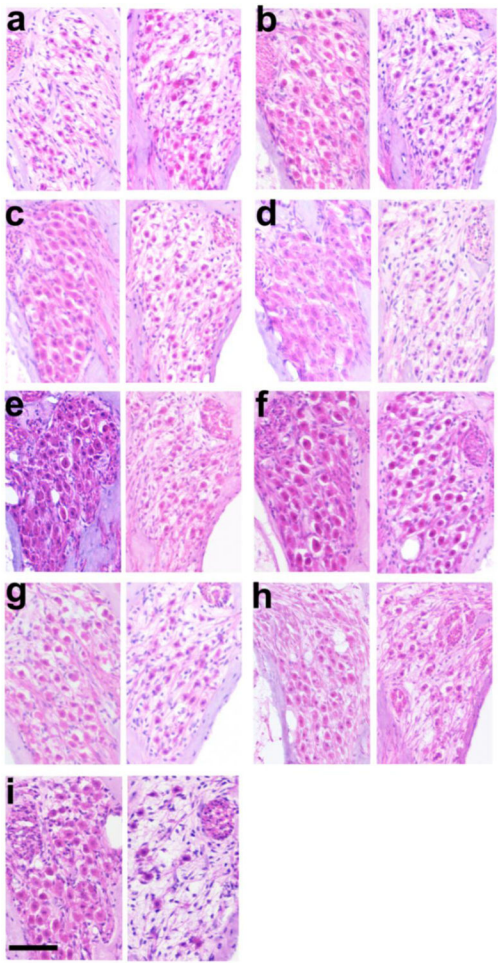

Figure 6.

Representative micrographs of Rosenthal's canal illustrating AN survival from the UB turn of the left (stimulated) and right (control) cochleae from each of the nine chronically implanted cohorts (Table 1). (a) Implanted unstimulated control; (b)100; (c) 200 at 1000 pps; (d) 228; (e) 267; (f) 267 AP; (g) 267 CC; (h) 400; and (i) 540 μC/cm^2/phase CC. There was often an increase in AN survival in the UB turn of the chronically stimulated cochleae compared to its contralateral control cochlea. Scale bar = 50 μm.

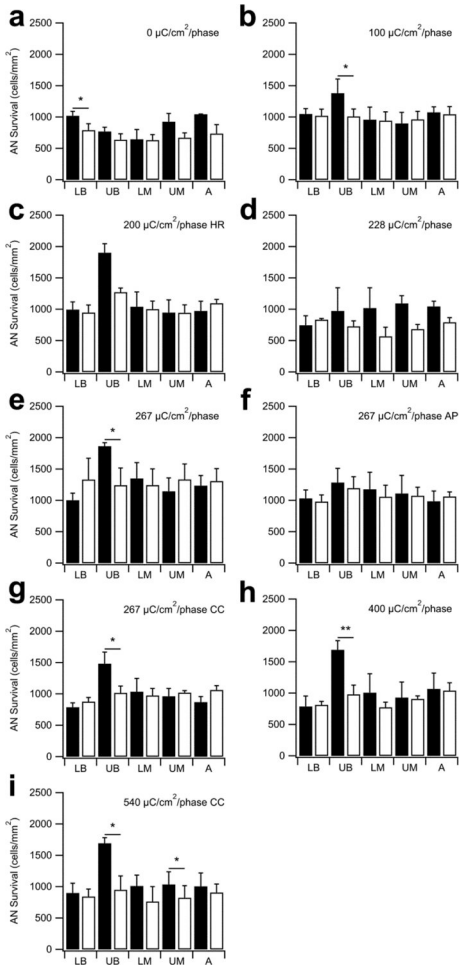

Figure 7.

Mean AN density for both the implanted and contralateral control cochleae for each cohort in this study (black bars = implanted; open bars = contralateral controls). AN density was significantly greater in the UB turn (i.e. the site of stimulation) in five stimulated cohorts compared with their paired control (b, e, g, h, i). There was also a statistically significant difference in the LB region of the unstimulated control cochleae (a) and the UM region of 540 CC μC/cm^2/phase (i). There was no statistically significant difference in any other region of control or stimulated cochleae (i.e. LB, LM, UM and A turns). HR = stimulation at 1000 pps; AP = alternating leading phase; CC = capacitive coupling. * $p < 0.05$; ** $p < 0.01$ (Paired t-test; Error bars = sem).

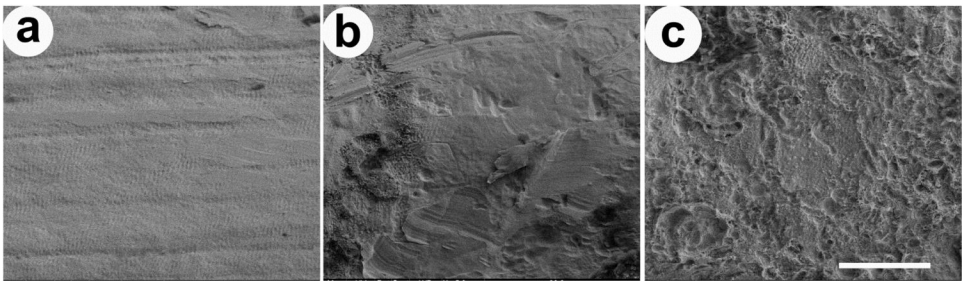

Figure 8.

SEM images illustrating the electrode surface of three Pt electrodes taken from an electrode array chronically stimulated at a level of 200 μC/cm^2/phase and 1000 pps (cohort 3; Table 1). (a) Electrode E1 was unstimulated and had a corrosion grade of 0. (b) Electrode E6 was a flanker electrode and had slight Pt corrosion (grade 2). (c) Electrode E7 was a centre electrode and exhibited extensive pitting corrosion across the Pt surface (grade 4). Scale bar = 20 μm.

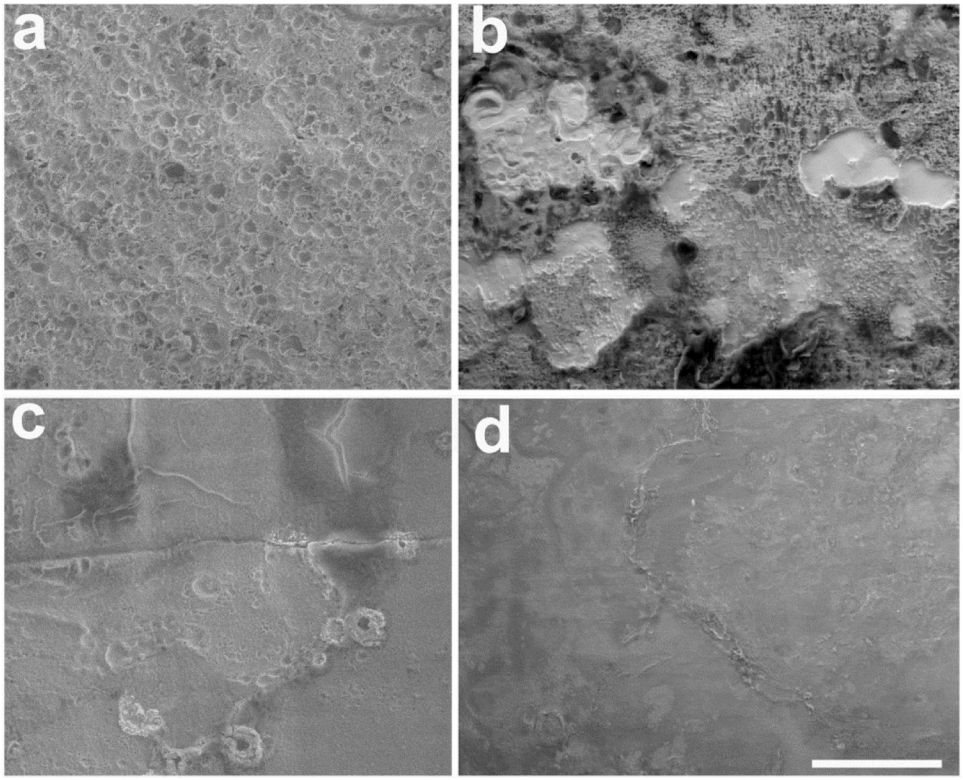

Figure 9.

Representative SEM micrographs of four centre tripole electrodes following chronic stimulation illustrating the effects of charge recovery on Pt corrosion. (a) Evidence of corrosion associated with stimulation at 267 μC/cm^2/phase using electrode shorting alone (grade 4) or (b) 267 AP μC/cm^2/phase (grade 3). In contrast, stimulation using CC at (c) 267 μC/cm^2/phase (grade 1) or (d) 540 μC/cm^2/phase (grade 1) resulted in far less visible Pt corrosion. All electrodes illustrated were stimulated at 200 pps. Scale bar = 20 μm.

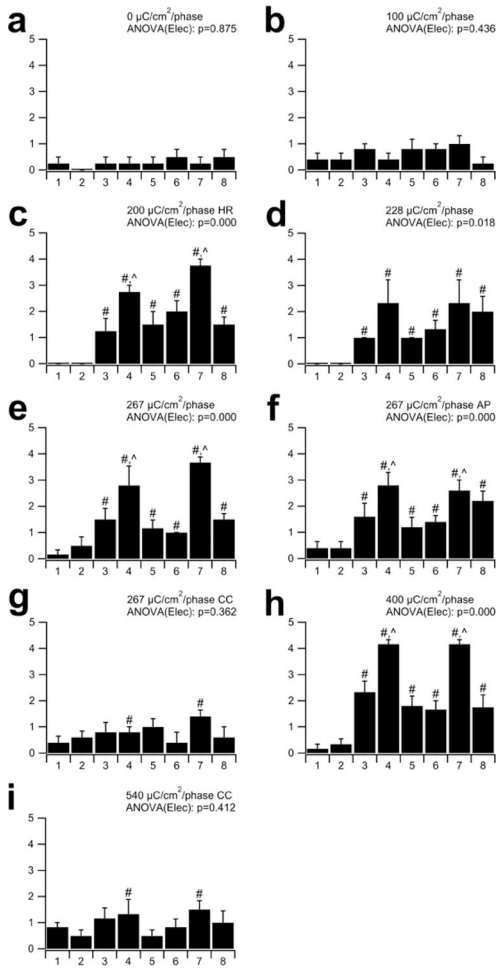

Figure 10.

Mean corrosion grade for electrodes E1–E8 in each cohort. There was minimal evidence of corrosion in the implanted unstimulated controls (a), electrodes E1 and E2 on the stimulated arrays, and all electrodes stimulated at 100 μC/cm^2/phase (b; grades 0–1). Slightly greater levels of corrosion were evident for the two CC cohorts (g & i) where the corrosion of centre tripole electrodes (E4 & E7) were significantly greater than all other electrodes on the array (#). More extensive corrosion was associated with electrodes stimulated at charge densities ≥ 200 μC/cm^2/phase using electrode shorting (c, d, e, h) or electrode shorting and AP (f). The degree of corrosion in these cohorts was most extensive on E4 and E7, while reduced levels of corrosion were evident on their flanker electrodes (E3, E5, E6 & E8). In some cohorts there was a significant difference between centre and flanker electrodes (Λ). HR = stimulation at 1000 pps; AP = alternating leading phase; CC = capacitive coupling. # = significant difference compared to unstimulated electrodes E1 & E2; Λ = significant difference with flanker electrodes E3, E5, E6 & E8. See text for details of statistics. Error bars = sem.

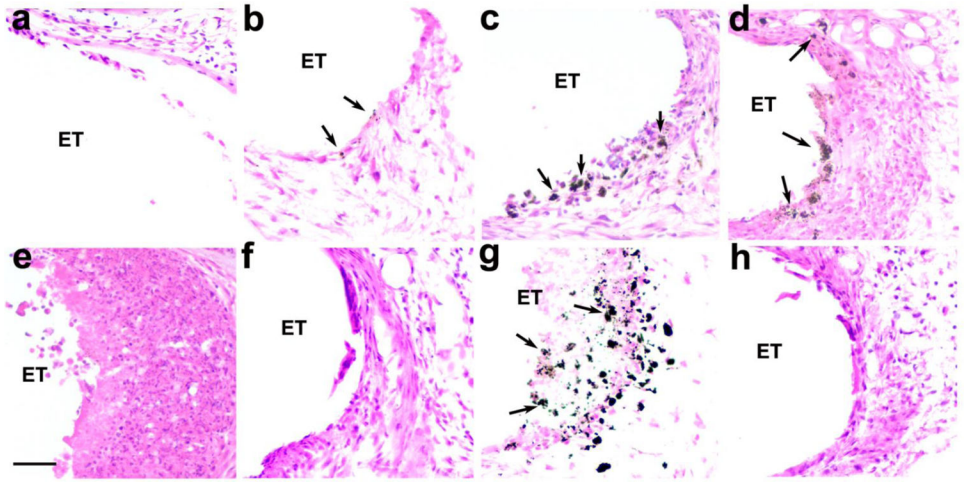

Figure 11.

Representative photomicrographs illustrating the electrode-tissue capsule (ET) in the UB turn of eight of the cohorts used in this study. The extent of the particulate deposits (arrows) appeared to vary with both charge density and the technique used to achieve charge balance. (a) Implanted, unstimulated control (cohort 1): (b) 100 μC/cm^2/phase with electrode shorting (cohort 2); (c) 228 μC/cm^2/phase with electrode shorting (cohort 4); (d) 267 μC/cm^2/phase with electrode shorting (cohort 5); (e) 267 μC/cm^2/phase with electrode shorting and AP (cohort 6); (f) 267 μC/cm^2/phase with electrode shorting and CC (cohort 7); (g) 400 μC/cm^2/phase with electrode shorting (cohort 8); (h) 540 μC/cm^2/phase with electrode shorting and CC (cohort 9). ET = electrode tract. Scale bar: 50 μm.

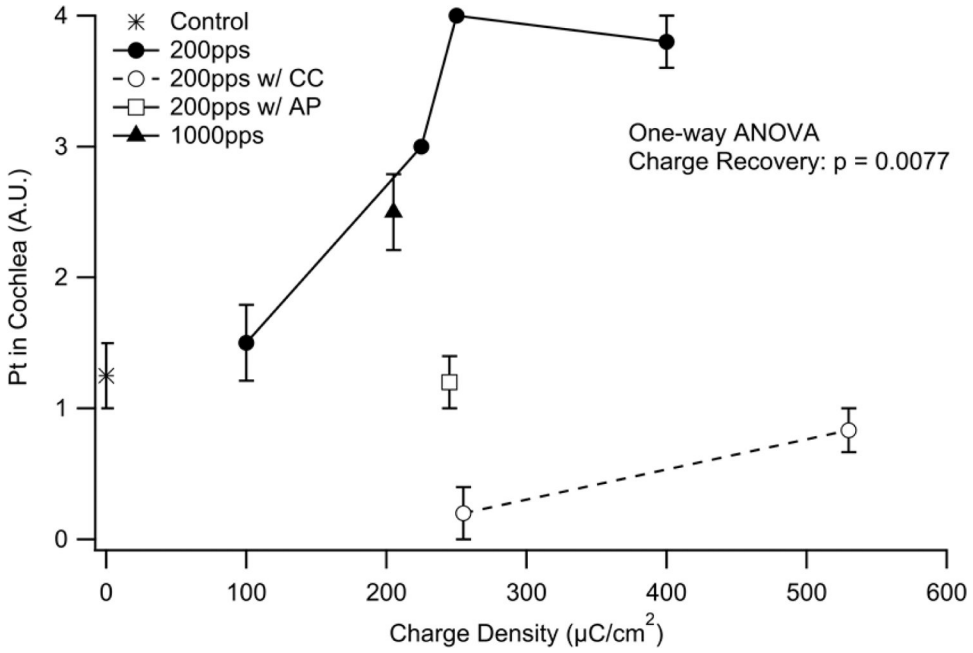

Figure 12.

Mean extent of particulate Pt occupying the UB turn scala tympani as a function of charge density. There was a statistically significant increase in Pt corrosion products associated with charge density ($p < 0.01$). The charge recovery technique also appeared to effect corrosion product ($p < 0.01$), with reduced levels associated with AP and CC. Error bars = sem.

Table 1:

Summary of the cohorts used in this study.

Cohort	Charge per phase (μC/phase)	Centre electrode* charge density (μC/cm²/phase) **	Flanker electrode charge density (μC/cm²/phase)	Charge recovery technique	Stimulus rate (PPS)	N (cochleae)
1§	0	0	0	N/A	N/A	4
2§	0.2	100	50	ES	200	5
3	0.2	200	100	ES	1000	4
4	0.2	228	114	ES	200	3
5§	0.2	267	133	ES	200	5
6	0.2	267	133	ES & AP	200	5
7	0.2	267	133	ES & CC	200	6
8§	0.2	400	200	ES	200	5
9	0.2	540	270	ES & CC	200	6

Notes:

*Unless otherwise stated, the cited charge density refers to that on the centre electrode of the tripole.

**Geometric surface area.

§Cohorts reported in (8).

N/A, not applicable; ES, Electrode shorting; AP, alternating leading phase; CC, coupling capacitor in series with stimulator output.

Table 2:

Pt trace analysis data for each stimulated cohort in this study.

Cohort	Stimulation parameters	ng/mg half cochlea
1	Implanted controls	1
2	100 μC/cm^2/phase; 200 pps	-
3	200 μC/cm^2/phase; 1000 pps	-
4	228 μC/cm^2/pnase; 200 pps	124
5	267 μC/cm^2/pnase; 200 pps	147
6	267 μC/cm^2/pnase; 200 pps; AP	88
7	267 μC/cm^2/pnase; 200 pps; CC	61
8	400 μC/cm^2/pnase; 200 pps	136
9	540 μC/cm^2/pnase; 200 pps; CC	93

Note: - = data not available